EPJ manuscript No.
(will be inserted by the editor)

The movement of a one-dimensional Wigner solid explained by a modified Frenkel-Kontorova model

W. Quapp[1], Jui-Yin Lin[2], and J. M. Bofill[3]

[1] Mathematisches Institut, Universität Leipzig, PF 100920, D-04009 Leipzig, Germany (ORCID: 0000-0002-0366-1408) e-mail: quapp@math.uni-leipzig.de
[2] Quantum Dynamics Unit, Okinawa Institute of Science and Technology (OIST) Graduate University, Tancha 1919-1, Okinawa 904-0495, Japan (ORCID: 0000-0001-8286-1004) e-mail: musicara@gmail.com
[3] Departament de Química Inorgànica i Orgànica, Secció de Química Orgànica, and Institut de Química Teòrica i Computacional, (IQTCUB), Universitat de Barcelona, Martí i Franquès 1, 08028 Barcelona, Spain (ORCID: 0000-0002-0974-4618) e-mail: jmbofill@ub.edu

Received: August 17, 2020 / Revised: October 5, 2020/ Accepted:

Abstract. We propose a Frenkel-Kontorova model for a 1D chain of electrons forming a Wigner solid over ^{4}He. It is a highly idealized picture, but with the model at hand we can study the movement of the chain. We find out that the energetically most preferable movement is the successive sliding of a kink or an antikink through the chain. Then the force for a movement does not depend on the length of the chain. The force uniformly applied to all electrons must be larger than a force exciting only a kink or an antikink. We calculate two cases, one with stiff 'springs' between the electrons and one with weak 'springs'. The side potential of the 'dimples' is additionally damped at the periphery. We study the cases with 33, 66, and 101 particles.

PACS. Quasi-1D electron systems – Winger solid – Frenkel-Kontorova model – Damped side potential – Newton trajectory – Langevin equation – Barrier breakdown point – Kink/antikink motion

1 Introduction

A Wigner solid (WS) is an experimental fact [1] that has first been observed in a system of two-dimensional surface-state electrons (SSE) floating above a liquid helium-4 surface [2,3]. Given that liquid helium is weakly polarized, the unscreened Coulomb interaction of electrons benefits a WS formation from SSE crystallization at densities of order $10^{13}\,m^{-2}$ and at temperatures around $1\,K$. The strong inter-electron interaction makes this SSE system an ideal system for studying many-particle problems [4–7] especially for the driven dynamics of strongly correlated systems.

Typical experimental devices for studying the driven dynamics of SSE on helium are similar to a semiconductor field-effect transistor [8,9]. Here SSE are capacitively coupled to the source, channel and drain electrodes beneath liquid helium. A pair of split gates on the liquid helium level is used to reduce the effective width of the channel, so that a quasi one dimensional (1D) configuration of SSE can be realized. Confining the SSE in capillary-condensed micro-channel structures is practical for investigating nonlinear electron transport and phase transitions. The strongly-correlated WS phase gives rise to many interesting phenomena, such as the re-entrant melting of quasi-1D electron crystals [10–12], stick-slip motion of a WS [13,14], the bistable transport properties of a quasi-1D WS [15], the finite-size effect of WSs on sliding transition [16,17], and the loss of the long-range positional order of a quasi-1D WS in the presence of an external periodic potential [18].

The competition between the collective behavior of the strongly correlated particles and the influence of the environment on individual particles is important for many-particle problems. The nonlinear transport properties observed in the aforementioned works essentially result from the strong coupling of WSs and the liquid surface. The soft liquid surface commensurately deforms with a WS due to the electrostatic pressure of the localized electrons of the WS, so that a 1:1 commensurate dimple lattice (DL) forms [19]. The profile of the DL deformation is composed of sinusoidal waves, and it was estimated for the WS of different velocities according to the hydrodynamic theory [20]. When the WS is at rest, a typical depth of the DL is about $10^{-12}m$ [20]. When the velocity of WS approaches the phase velocity of the surface wave with a wavelength that matches the WS lattice constant, the DL drastically deepens due to their resonance [21]. This resonant surface-wave emission from a WS is also known as the Bragg-Cherenkov scattering [22] which first explains the nonlinear WS driven dynamics with a strong coupling to the

quantum field of capillary waves [23]. While the DL deepens, the frictional force experienced by the WS increases at the same time. The coupling with varying profiles of the commensurate DL significantly influences WS's transport properties along the liquid surface. We assume here this strong coupled relation between the WS and the dimples.

At least, if one exposes the WS to an external electric field then the redistribution of the electrons can be recorded as a current [8,16,17,24].

We understand the WS as a chain of particles and report here on a numerical study of a 1D model WS. The site-up periodic substrate potential of the DL is assumed to be a sinusoidal function with its amplitude smoothly decaying to zero at the two ends of the DL. It is really of finite length. It represents the damped resonant DL with the boundary condition of a zero amplitude. We assume exponential decay of the DL at the boundaries, because the transient part of a general solution to a damped driven oscillators suggests a form of expoential decay. We search the form of the movement of a 1D WS through a site-up potential. Intrinsically there is no misfit between the WS and the DL. Under an external electric field we assume an immediate reaction of the electrons and a frozen surface deformation. We use the Frenkel-Kontorova (FK) model for the movement of the electrons. The model was explained and discussed in Refs.[25–27]. The FK model describes the situation of the 1D WS: a chain of particles with 'spring' forces in between is embetted in a site-up potential. We use here a modified Frenkel-Kontorova model, see Section 2.

All electrons subject to the Coulomb force. However, the electrons in both reservoirs before and after the channel of the chain, in the experiments [17,18], press the chain into a pattern with fixed distances. In a 1D-chain the Coulomb potential between electrons is screened by the presence of other electrons [28]. This is the ground assumption of the FK model. On the other hand, fixed boundary conditions for the particles p_1 and p_N of the chain would destroy an FK model of a finite, but freely moving chain [25]. So we leave free the boundary conditions of the chain, and it can move like in the experiment under an external electric field.

Overall, we treat here the potential energy surface (PES) for the N electrons of the experimental chain and search for low lying 1D valleys through the 'mountains' of the N-dimensional PES for a sliding of the WS chain. The method corresponds to studies of chemical reactions through the PES of the corresponding molecules. An important part of the theory is the use of Newton trajectories (NT) for the description of the moving stationary points of the PES under an external force. The NTs are curves in the configuration space of the chain. The NT theory was discussed in Refs.[29–32]. They are curves where at every point the gradient of the PES points into the same direction, called the search direction. If we compress or pull the chain, some or all coordinates of the electrons change. Some examples of a changed chain are drawn below. Because we can draw all N particles of a chain we can illustrate here N changing dimensions. Such events are described in depth by the NTs. Every point of an NT is a configuration of the chain. To a given driving force, the search direction, on any number of chain electrons, we get the 'static' curve of the NT on the PES of the movement of the chain. For practical reasons, we divide every NT into M nodes. The number of nodes used depends on the step length of the predictor of the NT program.

Under an additional external energy, the chain tilts. In a second, quasi-dynamical ansatz we study the movement of the chain on the tilted PES by a Langevin equation. If the tilting is large enough, the chain starts to slide downhill on its effective PES. A fundamental observation is that the sliding pathway does not cross directly the stationary points of the unperturbed PES. However, it often crosses ridge regions over the corresponding SPs in the valleys which we know by NTs.

We find that the chain never moves as an inelastic, 'solid' body, or with a 'collective sliding'. The chain of electrons in the drain of the experiment will be picked up by the external force (see Eq.(12) below). If the force is high enough then the chain forms a kink or an antikink. A kink is a stretched structure of a part of the chain where an antikink is its compressed counterpart. These are quasiparticles which move like a wave through the chain along a flat valley of the PES, and they affect so the recorded current measured in the experiment. The motion of the chain goes on by steps of the periodicity a_s by antikinks, and/or kinks, or combination of both. The form of the existence of a movement with low excitation energy is the forward sliding of antikinks, akin to the biomechanical motion of an earthworm or a caterpillar, or the backward sliding of kinks. In biology we find a combination of shrinking and tension of individual parts of the body of the earthworm or the caterpillar.

In recent measurements, Badrutdinov et al. [16] and Lin et al. [17] found the rather surprising fact that the amount of force for an external movement of a quasi 1D WS with more than 30 electrons does not depend on the length of the chain. We give here a simple explanation of this unconventional result, even by the emergence of kinks / antikinks. To start the movement one has to overcome the amount of the barrier breakdown point (BBP) on the way uphill to the former SP_1. The BBP is a shoulder on the effective PES of the tilting. It depends on the direction of the external force.

In our previous work [27] we found kinks in commensurate and in incommensurate lattices. But in this case of no misfit here, we find sliding antikinks, kinks or pairs of them doing the movement of the chain. It is in contrast to the meaning of ref.[33] where the authors claim that kinks are an indicator for incommensurate lattices.

In section 2 we introduce the FK model used in this paper. The remains are divided into two parts. Part I dis-

cusses a 'strong' case of the spring potential with N=33, 66, and 101 chain length in the sections 3 to 6, and in section 7 we add the conclusions for the case. Part II in contrast studies a weak spring parameter for N=33. In sections 4 and 9 we study the action of a Langevin equation. Finally we discuss the Coulomb force of the electrons and the use of the FK model, and give some further conclusions.

2 The modified FK model for a Wigner solid

$\mathbf{p} = (p_1, ..., p_N)$ represents the position of N discrete particles of a chain, here electrons of the Wigner crystal. The positions p_i are on a linear axis. It holds $p_i < p_{i+1}$. We treat a finite chain. The free end points of the chain determine the average distance $a_o = (p_N - p_1)/(N-1)$. It is determined by the density of the electrons. Between the repelling electrons we have the long-range Coulomb force [34–37]

$$F_C(\mathbf{p}) = \frac{e^2}{4\pi\epsilon_o} \sum_{1\le i<j}^{N} \frac{1}{(p_i - p_j)^2} \tag{1}$$

with e is the electron charge, and ϵ_o is the vacuum permittivity. Note that in the Coulomb ansatz we do not have a dependence on the a_o distance; this distance is determined by the density of the electrons in the experiment. The thermal motion of electrons in the liquid/gas phase is fast. If the electrons are in the solid phase, they move slowly so that the liquid ^{4}He surface can deform accordingly. If then the electrons are subject to an orthogonal electric field, $E_\perp$, they induce dimples with the same distance in between like the electrons. Thus the on-site potential of the dimples has the same periodicity, $a_s = a_o$. The lattice constant a_s of the dimple lattice is determined to be somewhat less than the distance of the first WS detection, $5 \times 10^{-7} m$ [2]. But the a_s is still large enough to assume that the electrons interact like point charges [2]. So to say, the chain of electrons is a quantum dot molecule. The energy of the dimples depth is approximated by

$$v = eE_\perp\xi = (1.6 \times 10^{-19})(7.5 \times 10^5)(5.2 \times 10^{-11} \tag{2}$$
$$= 6.2 \times 10^{-24}[Joule]$$

with the holding field, $E_\perp$, which presses the electrons into the He which is about $7.5 \times 10^5 V/m$ and the amplitude ξ is estimated to $5.2 \times 10^{-11} m$ [13]. The amplitude of the surface wave, ξ, describes the resonating ripplons of the He-surface.

The first aim is to coarsely approximate the Coulomb force by a harmonic force between neighboring particles. The first step is the approximation of the double sum in Eq.(1) by a single sum over only neighboring electrons just for the sake of simplicity. We get

$$F_C(\mathbf{p}) \approx \frac{e^2}{4\pi\epsilon_o} \sum_{i}^{N-1} \frac{1}{(p_{i+1} - p_i)^2} \ . \tag{3}$$

Two consecutive summands contain the same electron, say for example p_{i+1}, and we can look for the Taylor series for the variable p_{i+1} developed at the equilibrium distance, a_o,

$$F_C(\mathbf{p})\Big|_{i+1} \approx \frac{e^2}{4\pi\epsilon_o}\left(\frac{1}{(p_{i+1} - p_i)^2} + \frac{1}{(p_{i+2} - p_{i+1})^2}\right) \tag{4}$$
$$= \frac{e^2}{4\pi\epsilon_o}[\frac{1}{a_o^2} - \frac{2}{a_o^3}(-p_i + 2p_{i+1} - p_{i+2}) + O[2]\ ]$$

We suppress the first term, a constant, and the higher terms. We can use the linear term to look for a corresponding potential energy of the springs. We get the corresponding two summands containing the p_{i+1}

$$\frac{e^2}{4\pi\epsilon_o a_o^3}[(p_{i+1} - p_i - a_o)^2 + (p_{i+2} - p_{i+1} - a_o)^2] \tag{5}$$

and the sum over all electrons then results in the transformed 'harmonic' energy

$$S_H(\mathbf{p}) = \frac{e^2}{4\pi\epsilon_o a_o^3} \sum_{i}^{N-1} (p_{i+1} - p_i - a_o)^2 \ . \tag{6}$$

In the numerical tests we scale the a_s-constant of the dimples potential to 2π for computational simplicity. Because $a_s = 2\pi$ it causes a coordinate transformation

$$x_i = \frac{2\pi}{a_o}\ p_i, \quad i = 1, ..., N \ . \tag{7}$$

For the spring potential the transformation means

$$S(\mathbf{x}) = \frac{e^2}{2^4\pi^3\epsilon_o a_o} \sum_{i}^{N-1} (x_{i+1} - x_i - 2\pi)^2 \tag{8}$$

where the spring constant $k/2$ is the factor before the sum. As the result of the transformation we have instead of Eq.(1) a harmonic trap, $S(\mathbf{x})$, for the electrons by a nearest neighbor potential.

Additionally we fix the row of dimples including the damped ones. Thus we artificially exclude a moving DL by surface waves (ripplons) [38], or, in other words, we set the ripplon relative velocity to zero (rigid dimple model) [39,40]. A reasoning may be that the electrons move quite faster than the dimples under an external force because the effective mass of a dimple is typically several hundred times the electron bare mass [41]. Thus each dimple can be treated as a massive object. In contrast, the formation of the DL contributes little to the stability of the WS itself [41]. The aim is here to decouple the WS from the helium surface. The range is on the x-axis (0, 2π N) for the N dimples. In our calculations the chain can move by one or two dimple places further. The PES for the variable changes of the x_i is the modified Frenkel-Kontorova model

$$V(\mathbf{x}) = D(\mathbf{x}) + S(\mathbf{x}) \tag{9}$$

where D is the potential of the dimples and S is the potential of the 'springs' between the electrons with Eq.(8).

$$D(\mathbf{x}) = \frac{v}{2}\sum_{i=1}^{N}\begin{cases}(1-Cos(x_i))Exp(-(20\pi - x_i)/15) & \text{for } x_i < 20\pi \\ (1-Cos(x_i)) & \text{for } 20\pi \le x_i \le 2\pi(N-11) \\ (1-Cos(x_i))Exp(2\pi(N-11) - x_i)/15) & \text{for } 2\pi(N-11) < x_i\end{cases} \quad (10)$$

For N we use values ≥ 33 to save an internal part of the chain. In the first part of this paper we calculate N=33, 66, and 101. In part II we treat N=33.

The ratio of the constants of the two potentials becomes

$$\frac{v}{k} = \frac{8\pi^3\epsilon_o E_\perp \xi a_o}{e} = 0.27 \quad (11)$$

with Eqs. (2) and (8) where the units cancel. It is $\epsilon_o = 8.854\times10^{-12}$ F/m, $E_\perp = 7.5\times10^5$ V/m, $\xi = 5.2\times10^{-11}$ m, $e = 1.6\times10^{-19}$ C, $a_0 = 5\times10^{-7}$ m.

The uncertainties in Eq.(11) are the depth of the dimples, ξ and the distance a_0. They can variate under different conditions [42]. In this paper we treat two different models to take into account the uncertainties. First we fix in the potentials $v = 2$ and $k = 8$. The value $v = 2$ is used in the PES of $\mathbf{D}(x)$-figures in the next sections. Secondly we fix a ratio with another parameter k to study the action of the model under drastically changed relations. We use $v = 2$ and $k = 1$ in part II of this paper. The situation then changes to a stronger dimple potential, or a weaker string constant. However, we will see that the qualitative pattern of the existence of kinks or antikinks is similar, in both cases.

Because we treat a simple special case of the FK model with $a_s = a_o$ with no misfit between the two potentials, we immediately find the ground state of the chain with zero energy where all N electrons occupy N minimums of the dimples of the on-site potential.

Because $v > 0$, the on-site potential will modulate the chain if an external further force is applied. We use a linear force. We name the resulting PES an effective PES

$$V_F(\mathbf{x}) = V(\mathbf{x}) - F\ (l_1, .., l_N)^T \cdot \mathbf{x}\ . \quad (12)$$

The multiplication point between the N-dimensional normalized force direction vector $(l_1, .., l_N)^T$ and the N-variable $\mathbf{x}$ means the scalar product. F is the factor for the amount of the external force. The new term is often named dc driving (dc: direct current). The force tilts the former on-site potential for electron x_i with the incline $F\,l_i$, $i = 1, ..., N$. If the amount, F, of the force alternates then one names it ac driving [42]. The extremal points of the effective PES, V_F, move if F increases. It is described by NTs [29–32]. F increases to a maximum at the barrier breakdown point (BBP) [31], and it decreases again to zero at the next SP.

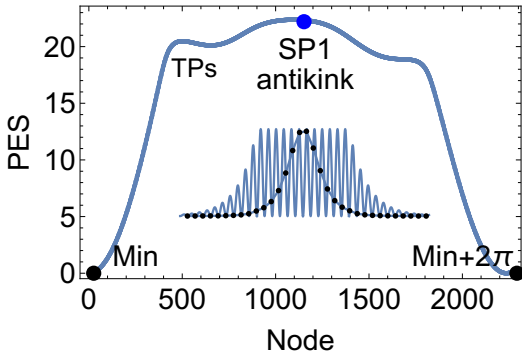

Fig. 1. The energy profile of an LEP over the antikink. The inset is the structure of the chain at the SP. Note that the electrons are artificially lifted on the dimples potential to guide the eye. The real chain is on a straight line. Only the distances can change.

3 PART I – THE STRONG SPRINGS – CASE v=2, k=8, N=33

3.1 A low energy path (LEP) for an antikink

There is an SP_1 of a symmetric antikink of the chain, a compressed structure. SP_1 means an saddle point on the PES of index one, with one valley-direction, but $N-1$ directions pointing uphill. It has two electrons in the full dimple 6 of the chain. They are compressed in the centre of the chain. Further electrons are sorted in the other dimples, one per dimple. So, the left half of the chain is moved by one dimple. We report on an NT over this SP which describes a low energy path through the PES in Fig.1. A mild turning point (TP) emerges before the SP_1 . Here the NT turns the increase of energy into a mild decrease. The search direction of the NT, $(l_1, ..., l_N)^T$, is the first eigenvector of the SP_2 of the PES, see subsection 3.3. The SP_2 direction is in between the two directions of the two SP_1, compare Fig. 5 below. The model of the chain is a very rigid one. Because of the large k-value the electrons form a stiff chain. It follows that the length of the antikink structure, L, is approximately the half length of the chain, $L \approx 16$. Thus, we cannot expect similar antikinks before or after this symmetric structure. And indeed, we only found this one SP_1 on this LEP. However, N=33 is even long enough to allow the antikink structure of the chain. The barrier of the SP_1 of the antikink is named Peierls-Nabarro barrier [43]. The PES of the SP_1-structure of the antikink has N eigenvalues of the Hessian matrix of the second derivations of the PES, $V(\mathbf{x})$ [25,44]. One eigenvalue is negative, the other $(N-1)$ eigenvalues are positive. This is the definition of an SP_1. The corresponding

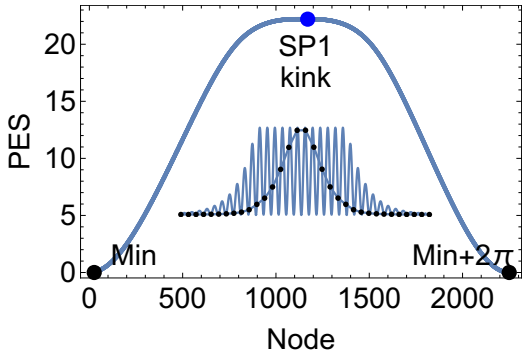

Fig. 2. The energy profile of the MEP over the kink SP_1. The inset is the structure of the chain at the SP. (To compare the structure with Fig. 1, see Fig. 4.)

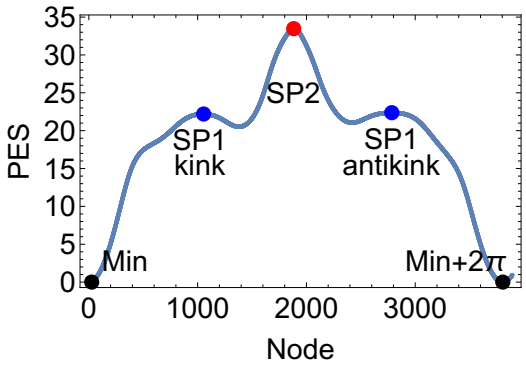

Fig. 3. The energy profile over an NT through three stationary points: the SP_1 of a kink, the SP_2, and the SP_1 of an antikink. A projected PES with all stationary points is shown in Fig. 5.

'negative' eigenvector points along the LEP over the SP_1. It is the 'decay'-mode of the SP_1. All other $(N-1)$ eigenvectors are orthogonal to the LEP at the SP_1. They point into the 'mountains' of the PES, and they have nothing to do with the movement of the chain along its axis over the LEP. The lowest four eigenvalues are 0.96, 0.22, 0.18, -0.06; thus there is not a phonon $\omega_{min} = 1$ like in ref. [45]. The reason may be the damped dimples used here. By the way, the term 'phonon' was coined by J. I. Frenkel [46].

3.2 The minimum energy path (MEP) for a kink

The minimum energy path is that with the lowest energy which we need to come through the mountains of the PES for a movement of the chain. A next SP_1 of a symmetric kink of the chain, a stretched structure, is shown in Fig.2. The chain has a gap in the full dimple 6 of the side potential. The profile is combined by the energy over two NTs. A unique NT for the pathway could not be found. The search direction of the left part up to the SP is the gradient of the barrier breakdown point (BBP) of the steepest descent from the SP back to the global minimum. This direction is mainly a pull direction. Similarly, the search direction of the right part down from the SP is the gradient of the BBP of the steepest descent from the SP to the other side to a moved minimum. Now the direction is inversely mainly a push direction.

Kinks and antikinks form the SPs of index one of the PES of the FK model. In section 3.3 we also cross an SP_2 of index two. For this chain with N=33 and flattened border dimples, a 1D pathway through the PES to a structure moved by a_s goes over one of the two SP_1, compare Fig. 5 below. There is no other pathway with comparable low energy. If we compare the two SP_1 of Fig. 1 and Fig. 2, we can say which one is the MEP, and which one is 'only' a low energy path.

Kinks are already studied elsewhere [45,47] for the simplest excited states which connect two neighboring ground states. In contrast to a remark in Ref. [45] we can give the exact shape of a kink by a numerical calculation, see Figs. 1 and 2.

It is worth noting that the kink, as well as the antikink form a spontaneous symmetry break of the given chain [48]. The two lowest eigenvalues, 0.21 and 0.209, of the ground chain are nearly degenerated. The two lowest eigenvectors, correspondingly, are a symmetric push, or an asymmetric push and pull, mainly in the outer regions of the chain. They point into the directions of the two LEPs of Figs. 1 and 2. The symmetry break for both LEPs is in a clear contrast to an assumption of a 'symmetry operation' in an FK chain in references [49,50]. Of course, the existence of kinks and antikinks in the FK model is long known, see for example ref. [51] and further references therein.

3.3 A pathway including the antikink and the kink SPs

The lowest SP_1 of the PES is a symmetric kink, a stretched structure. Many NTs which we tested go over this SP but then turn up to the SP_2 of higher energy, compare Fig.3. It depends on the direction of the applied force. The mirror picture of the symmetric minus-eigenvector of the SP_2 is used for the search direction. If the energy of the external electric force is high enough then the movement of the chain can also go over the region of the instable SP_2, however, any fluctuation will lead to a falling down of a real experiment to the next SP_1 valley. The structure of the three stationary points are given in Fig.4. The energy of the kink is 22.2, of the antikink, however, it is 22.37. The SP_2 comes to 33.38. This energy is near the sum of the height of all dimple-tops, because the springs are all near their equilibrium length.

The understanding of the localization of the three stationary points of the PES is possible by a projected PES into 2 dimensions. We use the two negative eigenvectors of the SP_2 as coordinate axes in the 33D coordinate space of all electrons. The eigenvector 1 is quasi symmetric with a small shift to more push. The eigenvector 2 is quasi asymmetric. The centre of a corresponding picture is the SP_2, and we name the axes s and a. The result is Fig. 5. The NT of Fig. 3 first climbs up to the lower SP_1 but it does not find the downhill path to the next minimum, however, it turns up to the SP_2. This is possible by the theory of NTs,

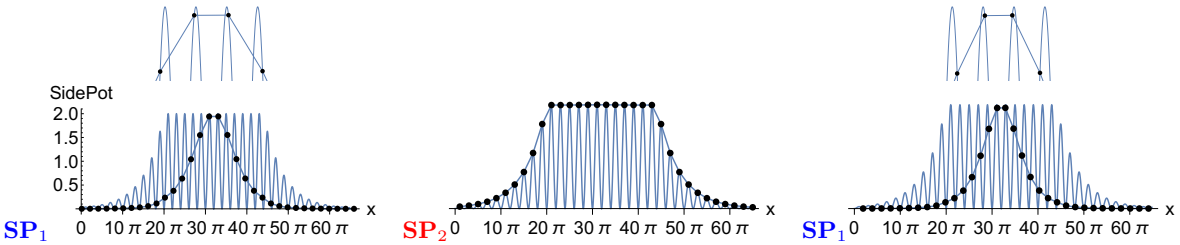

Fig. 4. The structure of the left SP_1 is a kink, the SP_2 is the structure of the chain moved by π to the tops of the dimples, and the right SP_1 is an antikink. The top of the central dimple 6 is enlarged, correspondingly to illustrate the difference of the two SP_1. A modified Frenkel-Kontorova model is assumed. In this model the 'y'-axis, the 'SidePot' is the energy of the dimples on the He surface with v=2. The spring potential is not illustrated.

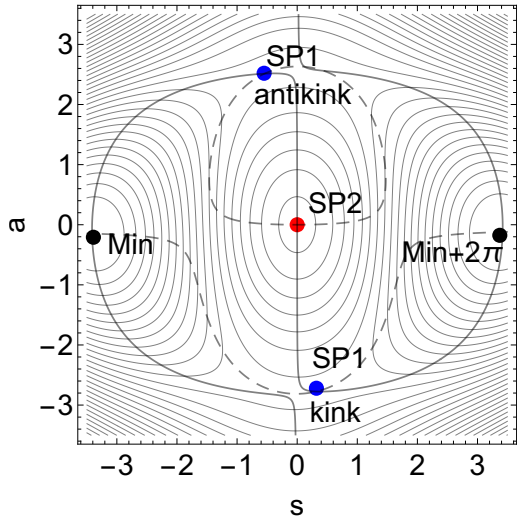

Fig. 5. The projected PES of the chain. Three stationary points correctly emerge near the a-axis for $s = 0$ – the low SP_1 of a kink, the SP_2 at the centre, and the upper SP_1 of an antikink. The solid line is the NT to direction a but the dashed curve is the NT to direction s.

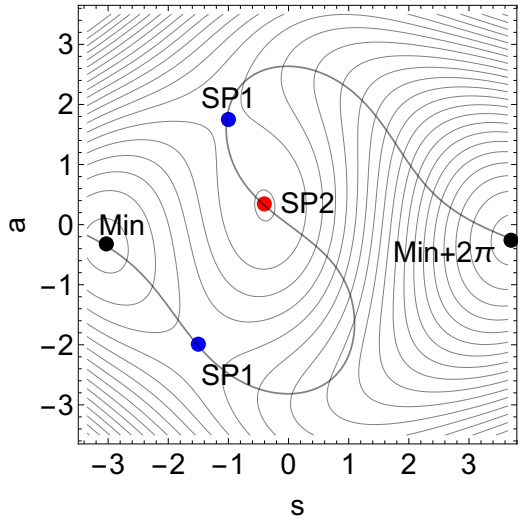

Fig. 6. The projected PES of the chain tilted by an external force (0.949, -0.316). The stationary points move on the effective PES along the NT (fat) to the tilting direction.

by the index-theorem [52]. Every NT connects stationary points with an index difference of one. So, also NTs to the SP_2 are possible. After the SP_2 the NT then goes down to the former SP_1 of an antikink, and finds the next minimum where the chain is again in the ground state but is moved by 2π.

One can understand the representation of Fig. 5 as the 2D pathway of the chain through its PES mountains. While the profiles of Fig. 1 and Fig. 2 describe 1D ways over the corresponding SPs of index one, the broad valley of Fig. 5 leads over the SP_2. The ridges on the left and on the right hand side of the 1D valleys have the dimension $(N-1)$ which may be imaginable. But at every point of the 2D valley we have ridges into the remaining $(N-2)$ dimensions. Of course these high-dimensional ridges are difficult to imagine.

The usual experimental external force direction, a fully equal external force, $\mathbf{f}=1/\sqrt{N}\,(1,...,1)^T$, also results in an NT similar to Fig. 3, see also Section 4.

We still discuss what a tilting would make with the PES using the example of this 2D projected surface. We apply the force $\mathbf{l}$=(0.949, -0.316) in Eq. (12) pointing to the lower SP_1. In Fig. 6 the corresponding effective PES is shown. The NT emerges if the amount F increases or decreases, correspondingly. Shown is the case F=1. The external force shifts the left minimum and moves together this minimum and the lower SP1. For a certain larger F, the two extremals will coalesce at the BBP. However, the upper SP_1 is moved uphill to the SP_2. Thus, the tilting causes a decrease of the lower barrier and an increase of the upper barrier.

Translated to the general case we can conclude that a force where the corresponding NT climbs up to an SP_1 in any case causes a movement of the chain to the new minimum. The arc of the NT over the other stationary points, SP_2 and the upper SP_1, only describes the 'background' of the process: when not included SPs move on the PES. It is not of interest for the chain itself.

Note that the NT (usually) does not describe the behavior of the chain. It describes the movement of the stationary points. If the chain is pushed, or pulled by the external force into the SP region, it will follow another, a

dynamical trajectory down to the next minimum, compare section 4.

Note further that we do not need to extend the amount of the force up to the BBP where the lower SP_1 and the former minimum coalesce. By a zero point vibration of the particles of the chain, or fluctuations, or noise, they will overcome a lower SP of a corresponding effective PES.

If the chain 'slides' down the effective PES into the next minimum, then it will submit energy. This energy could go to
(1) vibrations of electrons (temperature raises);
(2) take away due to cooling by the experimental environment;
(3) electron vibrations could induce off-resonant ripplons and modify the DL profile. This still needs further studies. If the chain is in the next global minimum, one dimple further, then a slip-stick cycle is finished, and the next can start. The cycle is consistent with a reported oscillation in an I V diagram of a WS transport [53]: "The oscillations arise from the switching between the pinned WS and a conducting state yet to be determined."

4 Dynamical sliding of the chain

We treat the equation

$$m\ddot{\mathbf{x}} + \eta\dot{\mathbf{x}} = -\mathbf{g}(\mathbf{x}) + F\,\mathbf{l} \qquad (13)$$

where on the right hand side the effective gradient of Eq. (12) is used. m is the mass of an electron and η is a damping factor. For FK chains with small mass of the electrons it is shown in Ref.[54] that we can use the case with m set to zero [41]. We can study an approximation of Eq. (13) by the overdamped Langevin equation [54]

$$\dot{\mathbf{x}} = -\mathbf{g}(\mathbf{x}) + F\,\mathbf{l}\,. \qquad (14)$$

Usually in experiments, one takes the symmetric force direction, $\mathbf{l}$=(1,...,1)^T. Start may be the global minimum. The force amount $F = 0.5$ is large enough to get a tilted effective PES where the chain slides downhill. Interesting is the pathway on the effective PES. For the solution of the differential equation (14) we have put the step length to 0.01 units, and get the profile of the steepest descent ansatz in Fig. 7. How we expect it, the sliding goes continuesly downhill, but with different slope.

To imagine the crossed structures of the chain, we have included two inlays in the figure. We additionally show a profile over the solution curve where the pure tilting part, $F\,(1,..,1)^T \cdot \mathbf{x}$, of the external energy is cut. This profile is shown in Fig. 8.

We find a strong increse of the former chain energy at the start: the search direction is fully symmetric, and after leaving the minimum region one is on a ridge of the PES. However, the steepest descent can go downhill on such a ridge. (Note it goes downhill on the effective PES of Fig. 7. Compare Ref. [55] where on a 2D PES a steepest descent crosses a ridge.) Steepest descent usually only bifurcates at stationary points, or before on a ridge by numerical effects. Here it goes up into the region of the SP_2.

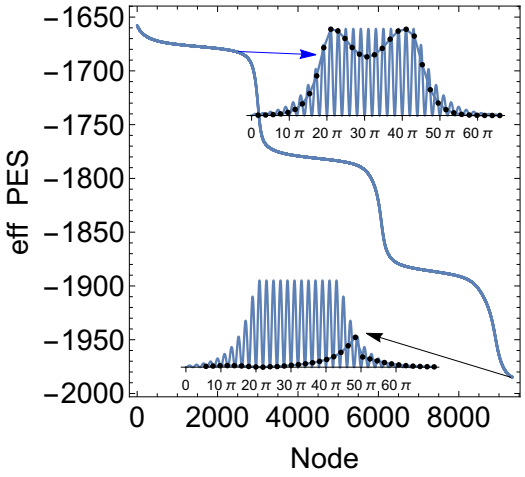

Fig. 7. The profile of the effective energy over a Langevin solution. The FK chain at the first shoulder is shown by an inlay, compare the SP_2 structure of Fig. 4, as well as the chain after the last step downhill.

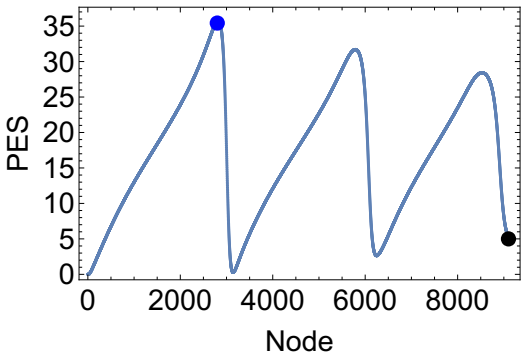

Fig. 8. The profile of the energy without the external part, over a Langevin solution. The two fat points depict the inlays of Fig. 7. The chain oscillates between the both structures under the sliding.

By numeric effects, in the next cycles the curve crosses the ridge somewhat befor the SP_2 region, and below, the curve touches a region near the minimum. Note that the last point shown is already moved along the site-up potential. The deflection of the energy profile is from SP_2 to global minimum. The MEPs are not met. The oscillation emerges because there are included 33 dimensions. If the MEP on the PES makes sharp curves from one dimension into another, what really happens, then the steepest descent 'cannot follow' such jumps immediately. Then it leads across a ridge.

In the cited experiments [17,18], however, one can assume that the symmetry of the dimples, as well as of the acting force, $\mathbf{f}$, is not perfect. Then the effective gradient in Eq. (14) will not strongly point to the fully symmetric SP_2, and one may get a profile with lower deflection than in Fig. 8, thus nearer to the MEP.

An NT to the same direction, on the other hand, follows a curve like the solid line in Fig. 5. So to say, it also leaves the MEPs and goes over the SP_2, however, in parts

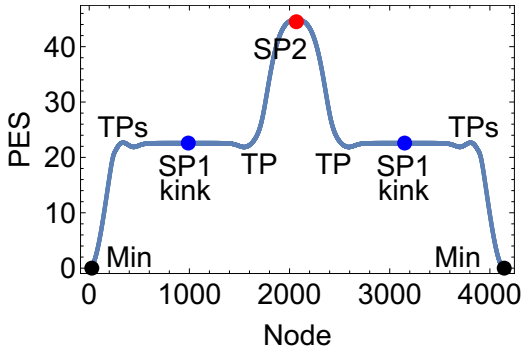

Fig. 9. The profile over the NT on the PES of the 66-chain to standard external force. Three stationary points again emerge: two SP_1 of kink nature and an SP_2 being a combined kink-antikink structure.

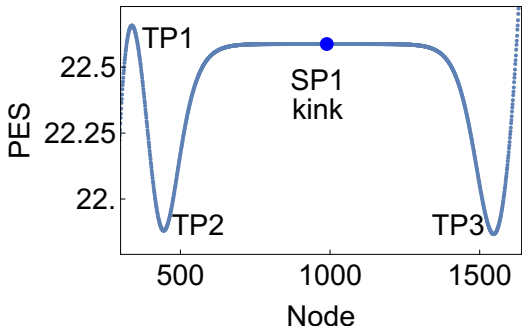

Fig. 10. Enlarged region around the left SP_1 of Fig. 9. The three TPs, and the SP are depicted in Fig. 11.

it goes along the MEPs and it crosses also the two SP_1 of the PES.

5 CASE v=2, k=8, N=66

We apply the usual experimental external force of equal components, $\mathbf{f}=F/\sqrt{N}\ (1,...,1)^T$. It makes a similar profile over the corresponding NT like in the shorter case before, see Fig.9. In the current case, the NT crosses the SP_2 and turns back to the same SP_1. It is possibly understandable by an analogy to the dashed NT in Fig. 5.

In Fig. 10 we enlarge the region of the kink-SP_1. The special points of the 66-chain are depicted in Fig. 11. Any excitation of the WS up to the SP_1 region in energy will result in a movement of the corresponding kink or antikink to the end of the chains central part, and then a 'falling down' of the structure to the next global minimum. This is a movement of the full chain by $a_s = 2\pi$. The energy of the kink is independent on the flat part of the path around the SP_1. This energy is 22.6 units.

A similar profile emerges with an antikink structure for the SP_1 if one uses another search direction, see Fig. 12. We take the second search vector of Fig. 2 and fill up the last 33 coordinates by zeros. The direction is then a push-direction for the chain. It causes the antikink.

6 CASE v=2, k=8, N=101

We treat the length of the chain of 101 electrons which is used in some experiments [17,18]. We find an analogous behavior of the two LEPs for a kink or an antikink like in the cases of $N = 66$ or $N = 33$ above. In Fig. 14 we show the energy profile over the NT to the standard search direction $(1,...,1)^T$. It makes the first floor for a kink, and an expedition to an SP of index two being again a pair of a kink-antikink structure. The SP_2 is shown in Fig. 15. Note that the kink has already slided to the left hand side of the chain, but again the NT goes a 'wrong' way up to the SP_2. A real excited chain would relax here at the TP before, and it would fall down to the next global minimum moved by 2 π.

Once more the second LEP also exists. The maximal antikink SP_1 central in the chain near $100\,\pi$ is again at 22.58780186846 energy units but a neighboring intermediate minimum is at 22.58780186041 energy units with a difference of 8.0×10^{-9}. The lowest eigenvalue of the SP is -1.14×10^{-7} and the eigenvalue of the minimum is 4.66×10^{-8}, thus this first 'floor' of the PES is flat. (More flatness cannot be.)

A similar flat floor we find for the sliding kink above.

Analogously to section 4, a test of the Langevin equation ansatz gives an impression of the possible dynamical behaviour of the chain. We set $\mathbf{f}=0.5\,(1,...,1)^T$, and the step length of the steepest descent 0.01, and get Fig. 16 for the profile of the solution on the PES without the external energy. The inlay is the structure at the brown point. It is a double kink with some further small excitations. Note that its energy is far below the global, full symmetric SP where all electrons are on the top over their dimples. The energy of the global SP is 169.4 units. The numerics of the Langevin equation anywhere departs from the fully symmetric path to the global SP and starts to oscillate in the region over the second floor. One can expect that in an experiment the conditions are also not fully symmetric so that a similar behaviour of the chain to Fig. 16 is to be expected.

7 Conclusions for PART I – the 3 cases with $v = 2, k = 8$

There are two 'parallel' low energy paths (LEP) over the PES near a level of 22.6 energy units, one for a sliding kink, but the other for a sliding antikink. If the external force is nearly optimal, what means that on its NT no TP emerges, and if this force is large enough to come to the BBP then the chain is excited to a lifting to one of these first floors. Because the floors are flat, an installed kink, or an antikink will slide over the PES to the other end of the corresponding floor – the antikink forward from the left hand side, but the kink backward from the right hand side of the chain. The next step is a back jump of the chain to the ground state structure, a minimum, but moving one dimple further by the distance a_s, here scaled to 2π. The

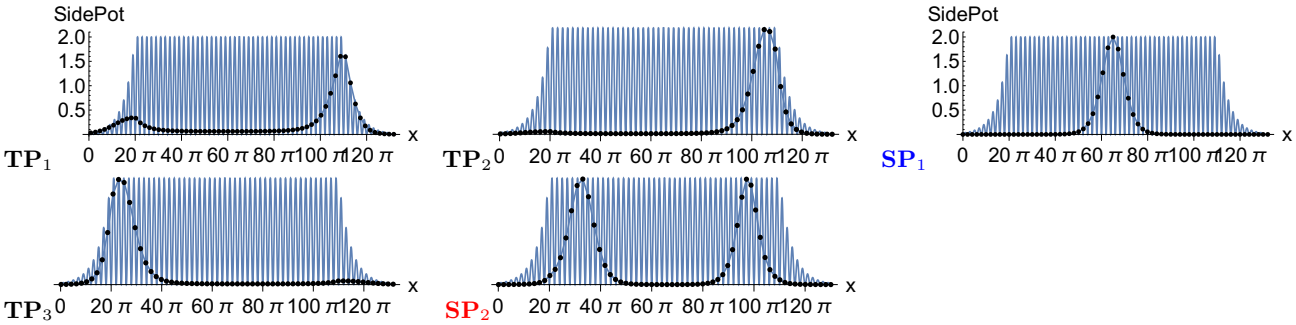

Fig. 11. The structure of the special points on the former profiles in Figs.9 and 10. The central SP_1 is a kink. The three TPs show how the structure develops along the NT. 'Unfortunately', the NT does not go down after the third TP to the new moved minimum, but it turns up to the SP_2. This SP_2 is a combined kink and antikink.

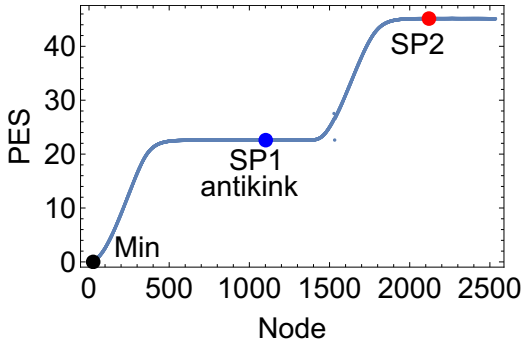

Fig. 12. The profile over a push-NT on the PES of the 66-chain. Similar stationary points emerge again. The SP_1 is now an antikink (see Fig. 13) and an SP_2 is again the combined kink-antikink structure, like in Fig. 11.

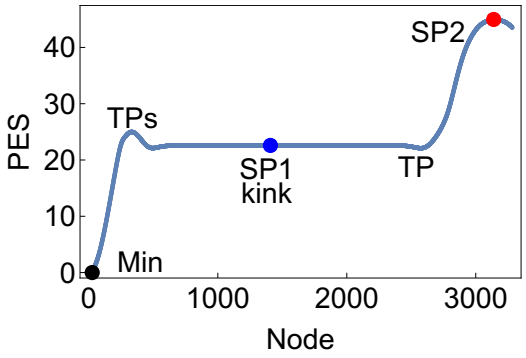

Fig. 14. The profile over the NT to the standard direction on the PES of the 101-chain. Similar stationary points emerge again. The SP_1 is a kink, and an SP_2 is again the combined kink-antikink structure, see Fig. 15.

stored energy of the chain will be radiated off. Then the next cycle will start. And so on.

Our result means that the formation of the kink, or the antikink, is the decisive step. The energy for this formation depends on the ratio v/k but not on the length of the chain. In PART II we discuss another k. Three different chains in PART I need the same energy for the rise up to their SP_1, thus to their move. This finding coincides with the results of refs.[16,17], see also Fig. 5 in [17] for larger N. Only for very short chains the amount of force is length-dependent. Then the length of the kink or antikink may be too long for the length of the chain itself, compare below Eq. (15).

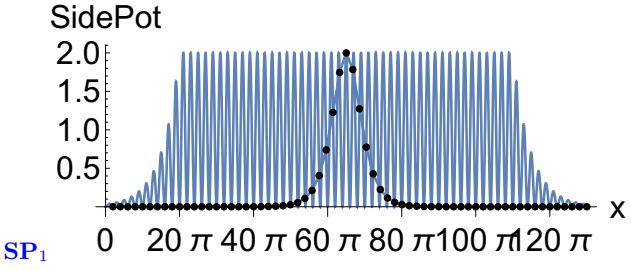

Fig. 13. The structure of the central SP_1 is an antikink.

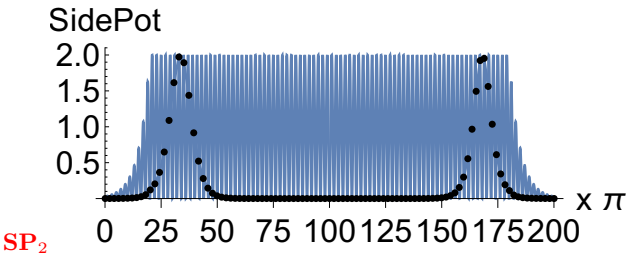

Fig. 15. The structure of an SP_2 for the 101-chain. Left is a kink, but right is an antikink.

Note that this model is in contrast to the assumption in other models that the chain moves as a whole [2,22, 41]. Thus here a substantial disagreement exists on the character of the motion. If one moves equally all electrons an $a_s/2$ step one gets the 'global' SP of the chain. Its energy linearly increases with the length of the chain. The 101-chain comes to an energy of 169.4 units and it is an SP of index 10 – quite higher than the SP_1 on the first floors of 22.6 units of a moving kink or an antikink. One could compare it to the SP_2 in Fig. 4. We guess that the real physics of the chain will go the much lower pathway on the PES under any excitation. Only a fully inelastic chain will move over this SP_{10} – it means that spring parameter

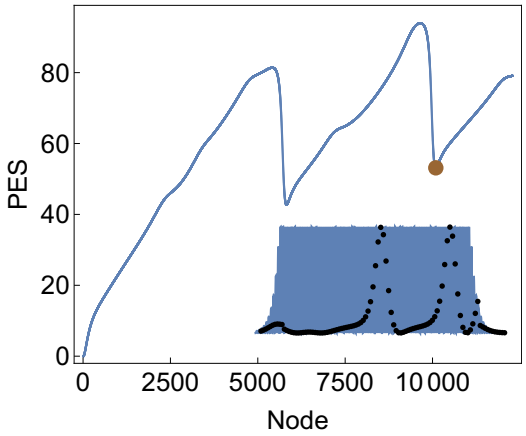

Fig. 16. Profile of a Langevin solution for the 101-chain for the pure PES part. The structure at the brown point is given by the inlay. It is a double kink with some further small deviations.

k becomes 'infinitely' large. In reality, however, the WS is not so solid. It is easy to perturb [1].

We thus understand the movement of the chain by single steps for successive dimples. The movement is done by sliding kinks or antikinks like the movement of an earthworm. After every step we are back in the ground state.

The main step always is the formation of a kink or an antikink. Its sliding along the tops of the full dimples then will go on 'automatically'. This may explain the experimental fact of the observation that a sliding of the chain is nearly independent on the length of the WS [16,17]. The movement also does not take place by any kind of an 'avalanche' [56].

Of course, if the excitation energy of the external force is higher than two times the first floor, then pairs of a kink and an antikink can emerge. For still higher energies a third floor can open, and so on. Then corresponding processes may become more complicated [51], see the next PART II for an example.

We do not discuss the relation of kinks to the lowest eigenvalues of the ground state of the chain. Under the SP_1 height of 22.6 one would get a lot of vibrational states before the level of the SP_1 named phonon modes [43,45]. Of course, most of these states are orthogonal to the MEP-direction. Because we will understand an excitation of the WS by an external field we do not need to speculate over excitations of diverse phonon modes.

8 PART II – THE WEEK SPRINGS – CASE v=2, k=1, N=33

8.1 The path for an antikink

By the much lower parameter, k, in comparison to Sections 3 to 6, we can expect that the PES of the chain changes qualitatively. It is an Aubry-trans-formation [57] – compare also a low dimensional explanation in Ref. [25]. The undamped case for k=1 was studied elsewhere [27] for N=10 and N=20. Here we find that the damped dimples model distinctively exhibits different properties from the pure FK model.

One MEP here is that of an antikink, which 'slides' through the PES, see the extended Fig. 17. The corresponding flat PES-level of the former SP_1 in PART I is now somewhat divided into a row of SP_1 and in noticeable intermediate minimums in between. But the kink- or antikink structures of the chain are much shorter, and its energy is much lower. This is caused by the lower springs between the particles. The first SP indeed starts at the main peak 2 of the upper line of the undamped dimples. At the first dimple maximum still exists a shoulder (Sh) of the PES.

The MEP across the PES with the level of one antikink is given in Fig. 18. We have composed it in four parts. The first part is an NT from the global minimum to the direction of the gradient in a BBP of the steepest descent from the first left SP (from full dimple 2 to 3). A further part 3 is an NT started at the central iMin in full dimple 6 to the 1st EV of this minimum. Part 2 is calculated with the mirror picture of the search direction of part 3, and part 4 is calculated with the mirror of part 1. Note that different pieces of this curve 'meander' through different dimensions of the configuration space of the chain. It emerges here as a plain projection.

We guess that a full sliding of an antikink along the MEP on the first floor can be realized by a combination of two NTs to alternating directions, see Fig. 19: the first part (in blue colour) is the NT to direction $(9{\times}0,\ 5{\times}1,\ 19{\times}0)^T$ - here named a push direction. It is stopped at 9 energy units. Note that such an excitation with an increasing energy over the NT describes the movement uphill of the last stationary point, an SP of index one. Thus the structure of the chain would change here to an additional next kink or antikink and not move further to a global minimum shifted by one lattice site, $a_s = 2\pi$. The second part (in brown colour) begins at the antikink in full dimple 5 near the centre of the MEP to the mirror direction $(19{\times}0,\ 5{\times}1,\ 9{\times}0)^T$ - now a pull direction. In the first case the force acts to the front of the central particles but in the second case the force pulls at the end of the central particles of the chain.

The further, right side of the blue curve increases along the slope of the PES. It is not shown here. Analogously, further into the left hand side of the brown curve, they would also increase uphill on the PES.

If one imagines the exact timing of such an ac drive between the two NTs along the ansatz of Eq.(12) with an amount, F, not exceeding the SP energies of the first floor then it will move the chain by one step a_s thus here by 2π. If then the next cycle starts it can again move the chain by one step, and so on, with an energy amount of the lowest floor only.

Fig. 19b opens the possibility to move the chain as a whole structure with low energy. The movement as a whole is composed by a moving antikink through the chain sug-

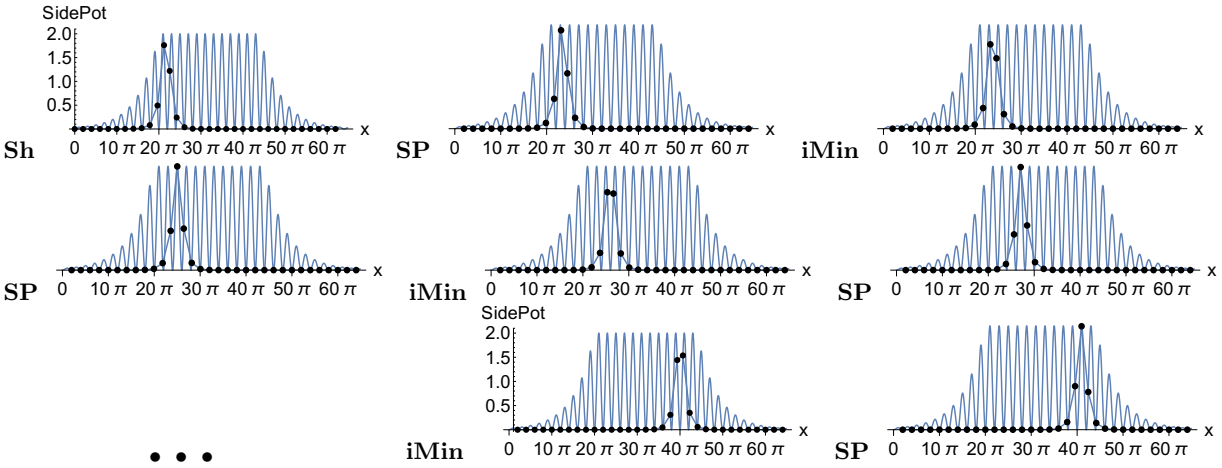

Fig. 17. Alternating SPs of index 1 and intermediate minimums of a chain with 33 electrons and k=1. The above left structure is a shoulder on the slope of the PES, with one eigenvalue zero. It is no stable structure. In the row, an anti-kink wanders over the MEP on quasi equal height from the left hand side to the right. There are in sum 10 SPs, and the length of an antikink is ≈ 5 electrons. The energy level of the SPs is ≈7.89 units, and of the intermediate minimums is ≈7.86 to 7.87.

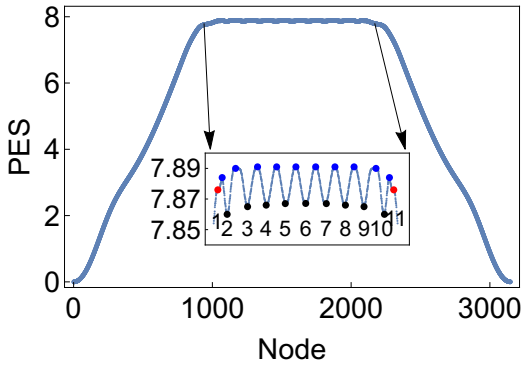

Fig. 18. The MEP of a 'sliding' antikink. The inset is an enlargement of the top of the pathway. The shoulders are red bullets, blue bullets are the SPs, and the intermediate minimums are black bullets. The numbers are the full dimples where the corresponding antikinks residue, compare Fig. 17.

gested by the consecutive panels of Fig. 17. At the end the chain has moved by one dimple-place.

8.2 Another MEP for kinks

There is a second kind of an MEP where a kink emerges at the right end of the chain and wanders through the PES in the inverse direction. The energy profile over only a single NT is shown in Fig. 20. The search direction for the NT was a vector with 7 zeros, 19 ones and again 7 zeros. It was inspired by an 'equal' force to all electrons. But a full vector with 33 times '1' does not work well, see below Sect. 9. We show the structures of some kinks in Fig.21.

Here the beginning of the MEP is a kink, a stretched structure, at the right end of the chain. Because the kink is a stretched structure, it wanders from the right end to the left end, in contrast to the antikinks of Fig.17 which wander from the left hand side to the right hand side.

Analogously to Fig. 19 one could guess for a still better ac drive of the full chain along its axis. Fig. 22 shows the energy profile over extended NTs of Fig. 19. The pathway goes from the 1st floor of antikinks, starting in the full dimple 6, to the 1st floor of kinks, up to the full dimple 6, and then alternating to the next beginning on the floor of antikinks. Such an ac drive would alternately push an antikink through the chain, then pull a kink through the chain, then again an antikink and so on.

8.3 The second floors

Another energy level is reached if two antikinks, or a kink and an antikink, or two kinks are in the chain, see Fig. 23. Then the energy level is quasi doubled, and we climb up to the 'second floor' of the PES. There are very many possibilities of the combinations of two such structures, into the different full dimples of the chain.

First we follow the NT to the unsymmetrical direction $(7\times0,\ 8\times1,\ 18\times0,)^T$. It pushes an antikink into the chain at the early beginning, and drives it up to the full dimple 9, compare the similar (blue) NT in Fig. 19a. After the antikink in full dimple 6 TPs emerge on the NT; because the NT is not simple a connection of the stationary points on the MEP. The different stationary points of the 1st floor go up to node 5700 in Fig. 23. After the iMin in full dimple 9, at least, emerges a high TP near 18.5 units and after that the NT finds a pair of two antikinks on the 2nd floor, see Fig. 23. The pair is the former antikink in full dimple 9 and a new one in full dimple 1. Because now two times an antikink was created, the left periphery of the chain is moved by two times the a_s length, here 4π. From here one can follow the NT on the 2nd floor. The new left antikink wanders up to full dimple 4 but then the NT turns back and at the end it jumps down near the old single antikinks on the 1st floor, exactly to the next SP between the full dimples 9 and 10. This is near node 13000 in Fig. 23. Interestingly one can continue the NT and in a next jump

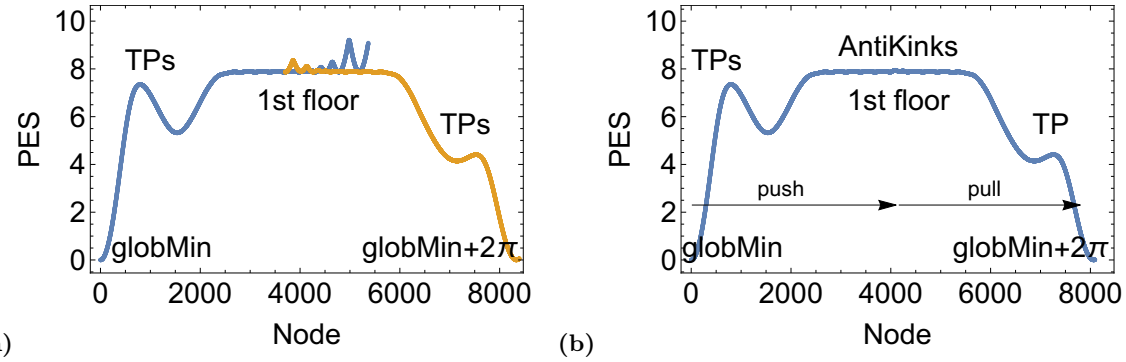

Fig. 19. (a) Two NTs which describe in parts the MEP for moving antikinks. The first one in blue is to search direction (8×0, 7×1, 18×0) thus a push-direction, where the second, the brown one is to pull direction (18×0, 7×1, 8×0). They overlay at the centre of the MEP. (b) Energy profile over the two combined NTs which are cut and now exactly meeting at the antikink in full dimple 6. The NTs act for a 'sliding' antikink over the full MEP, see text. It could be realized by an ac-kind of the excitation force.

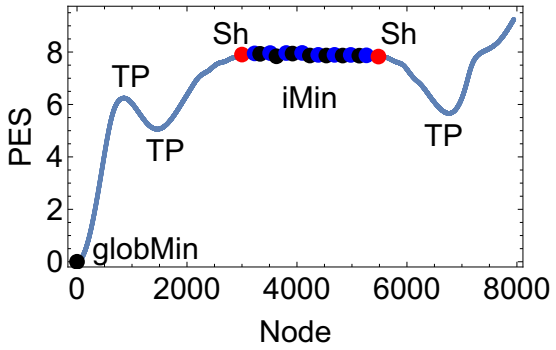

Fig. 20. Energy profile over an NT of a 'sliding' kink. The shoulders are red bullets, blue bullets are the SPs, and the intermediate minimums are black bullets. SPs and iMins alternate like in the former case of antikinks. The profile is drawn over only one NT. The pieces between the two TPs near node 1500 on the left hand side and node 7500 on the right is quasi the inner part of the MEP. Note that the final piece of the NT does not find its way down to the next global minimum, but it deviates uphill into the mountains. If one imagines here a shut down of the force in an ac-kind, after the right shoulder, then the steepest descent will lead to the next global minimum.

uphill it creates an SP-kink between the full dimples 1 and 2. Thus a pair kink-antikink emerges. But because now the push force has created a kink, the first particle of the chain is again back in its first (damped) dimple. The former movement of the left periphery is cancelled. On the 2nd floor of the mixed pair the NT again moves the kink into the centre of the chain. But again the NT turns back and jumps down to the 1st floor into a new antikink in full dimple 10. The game here starts again for pairs of two antikinks on the 2nd floor after node 22000. At least, the NT jumps back to a last structure on the first floor, an SP-antikink between the dimples 10 and 11 – near to the right damped periphery. After that, unfortunately, the SP-antikink does not flatten out, and does not move the chain into a new global minimum; no, the NT again rises up to the 2nd floor. But for the next pair of a kink and an antikink now the convergence of the NT finishes. This only-push direction used here does not deliver a strategy to move the full chain.

It seems tricky to propose a strategy for an ac driving of the chain to enforce a movement of the whole chain using these parts of the 2nd floor. In contrast, we guess that an external excitation energy for or over the 2nd floor will destroy the simplicity of a moving kink, or an antikink, on the first floor.

We show in Fig. 24 again an energy profile over an NT. It starts in a symmetric 'double'-SP, which is here only of index 1+1/2 because one of the eigenvalues is zero. It is structure 1 in Fig. 25. The search direction of the NT is the eigenvector to the zero eigenvalue.

Structures of stationary points along this NT are shown in Fig. 25. One could assume that there is not only one LEP over this second floor of the PES, however, a net of such pathways will exist. Additionally, there are NTs which connect SPs of the upper floor to structures of the first floor, the MEP.

8.4 Mixed pairs on the second floor

An NT to the symmetric direction $(12\times0,\ 9\times1,\ 12\times0)^T$ finds the second floor of mixed pairs of a kink and an antikink directly, see Fig. 26. Such a kind of pair production one can imagine also in a larger chain of particles when the force points to a special inner part of particles. It does not go over the outer regions of the chain where the dimples are flattened. The energy profile of the NT is shown in Fig. 26a, and some structures in Fig. 27.

Here the kink emerges on the left part of the chain, but the antikink is built on the right part. If the two structures wander through the chain so that the kink goes left and down to flatten, and the antikink goes right and down to flatten, then the chain would also move to the right hand side. In our case the NT goes into the other direction and again flattens out the structures at the end (not shown in the Figure) of the original global minimum.

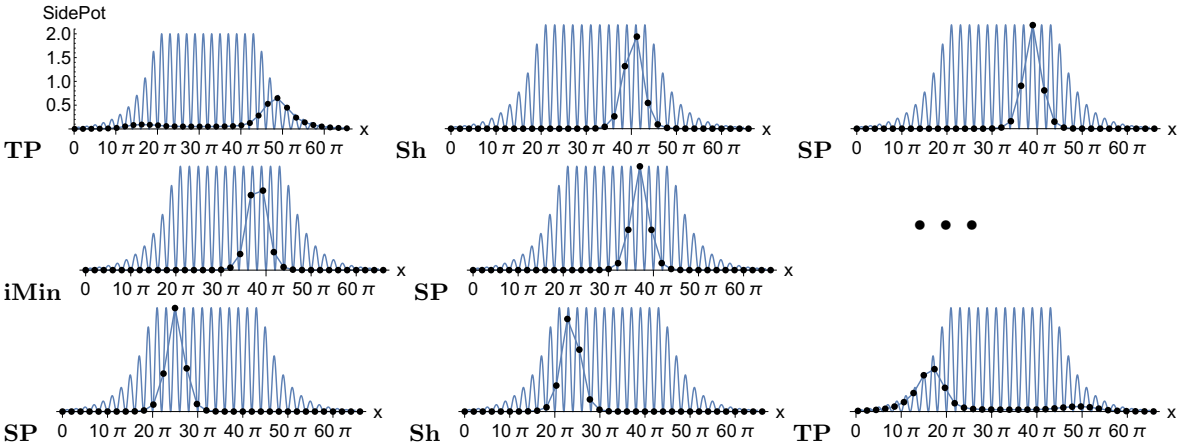

Fig. 21. The structure of iMin-kinks and SP-kinks along the top of the MEP of Fig.20. Additionally is shown the structure of the chain at two TPs of the NT at the beginning and at the end of the path.

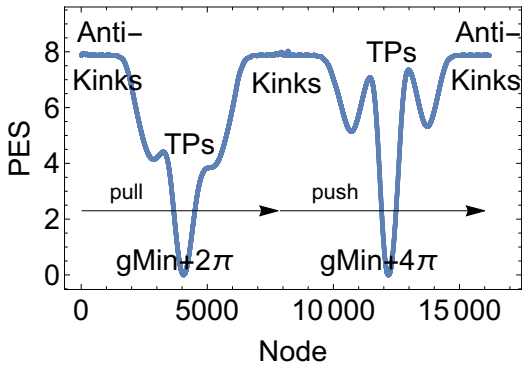

Fig. 22. Energy profile over NTs which go from the 1st floor of antikinks to the 1st floor of kinks and further to the next antikinks with a speculative ac drive, see text and compare Fig. 19.

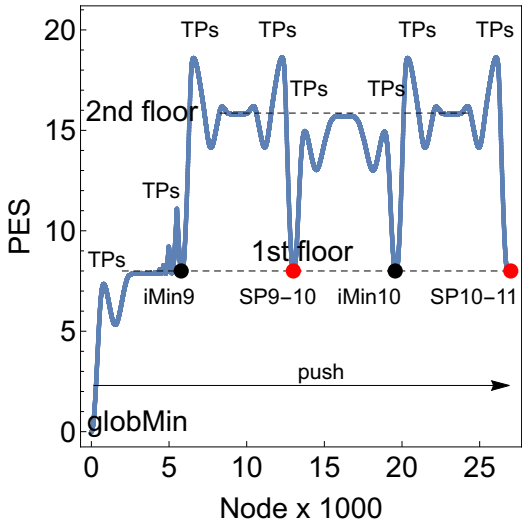

Fig. 23. Energy profile over an NT rising up from the 1st to the 2nd floor of the PES, and vice versa. Pairs of 2 antikinks wander on the left and the right pieces of the 2nd floor, but on the central piece are pairs of a kink and an antikink, see text. The symbol iMin9 means an antikink in full dimple 9, and so on.

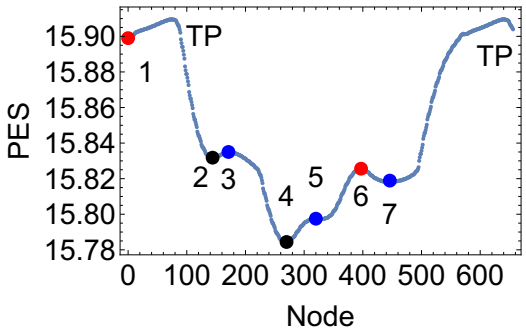

Fig. 24. Energy profile over an NT on the second floor of the PES. The stationary points are two antikinks. SPs of index 2 are red, usual SPs are blue, and the intermediate minimums are black.

In Fig. 26b we present a 'cyclic' NT to the unsymmetrical search direction $(9\times0,7\times1,0,7\times\text{-}1,9\times0)^T$. It would infinitely often turn through four different stationary points. By a corresponding exact ac-drive one could 'march on the spot'.

NTs to different search directions reach pairs of kink – antikink structures. Mainly the inner particles are to push by the external force. Then such a pair emerges inside the chain but the outer regions are unchanged. The NTs which climb up to the second floor do not lead, in the general case, to a movement of the chain as a whole. Such an NT meanders over the second floor and sometimes, it is mirrored and goes back, or it falls back to the ground level by unification of the pair, thus its annihilation.

8.5 Compare the two first 'floors' for kinks, or antikinks

In the configurations space of the chain, the family of kinks of the 1st floor, and the family of antikinks of the other 1st floor, reside in different regions. One could question some possible connections, over the second floor of kink-antikink, or antikink-kink pairs.

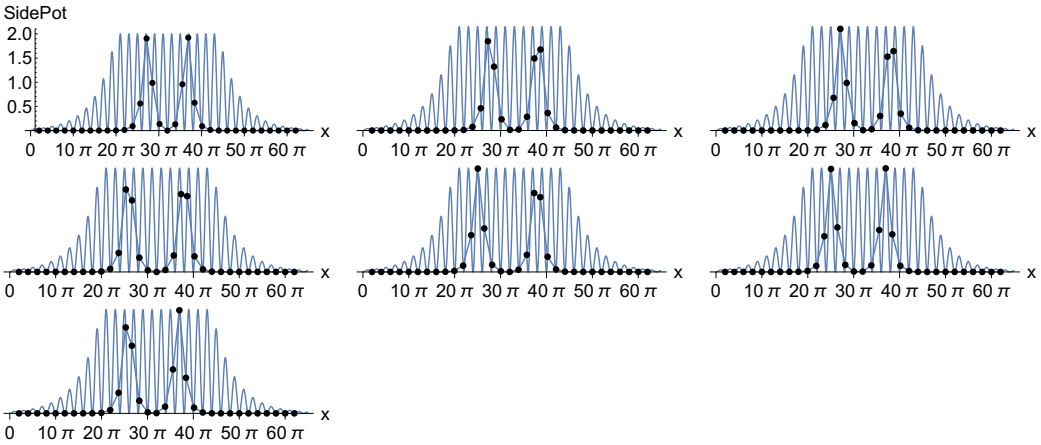

Fig. 25. Structures of the chain to points 1 to 7 (from left to right, and from top to bottom) of Figure 24.

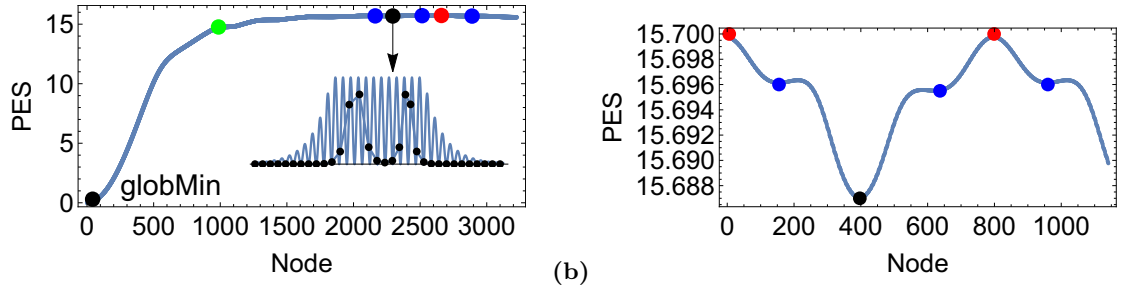

Fig. 26. (a) Energy profile over an NT up to the second floor of the PES. A BBP point is green, an SP of index 2 is red, usual SPs are blue, and an intermediate minimum is black, see Fig. 27. The iMin structure is shown in the inset. (b) Profile over an NT on the 2nd floor of pairs of kink-antikink structures which turns in a periodic run around a circle through four points: one minimum, one SP of index 2, and two SP_1.

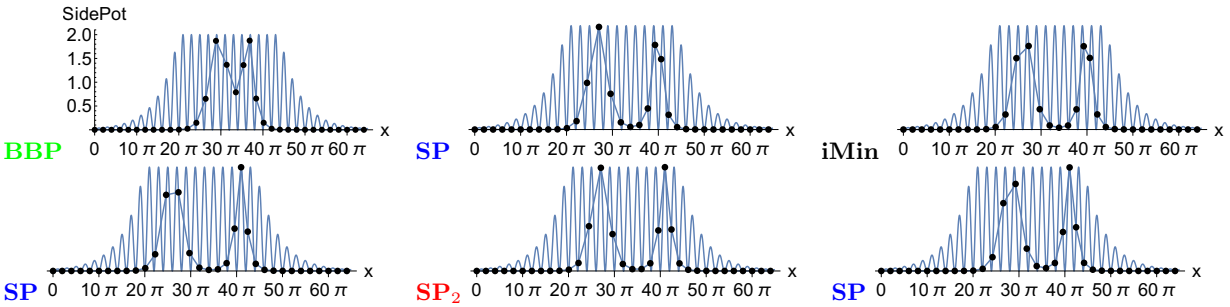

Fig. 27. Structures of the chain at a BBP (green) point and to the next stationary points of Figure 26(a).

A speculation could be that the central structures, where the kink is in its full dimple 6, or the antikink is in its full dimple 6, are the nearest neighbors. However, the midpoint of the two structures is exactly the SP_7 of the 'global SP', see Figure 28. This is because the two SPs are already differently moved: the antikink is on the left hand side moved out of the 'zero dimple' but for the kink the right particles are moved one place to the right hand side. Every pathway for a movement will circumvent this SP_7. Thus, from the point of view of the energy, one should look for other, nearer neighbors.

Note that the SP_7, the 'global SP', was in the previous Section 3.3 for $k = 8$ an SP_2 only. It really shows that the parameter k makes an enormous qualitative change of the 'combined' PES of Eq. (9).

8.6 Higher Regions of the PES

Higher regions of the PES are of importance for the dynamics of the chain in experiments, compare section 4. We report a result of NTs which find the 3rd floor, and the 'global' SP_7 where all particles are on top of the side potential, in analogy to the SP_2 of Fig. 4.

The NT to the unsymmetrical direction $(19\times0,\ 5\times1,\ 9\times0)^T$ (compare subsect. 8.1) starts at the global minimum, runs through the kinks of the first floor, rises up alternately to the second floor with kink-antikink pairs,

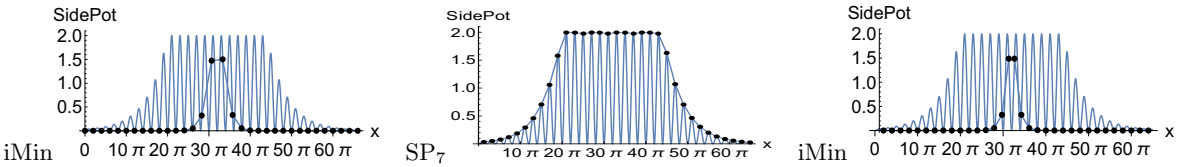

Fig. 28. Central structures of the chain at full dimple 6: kink left, antikink right, and the midpoint in between is an SP of index 7 of a forbidden high energy of 35.442 units.

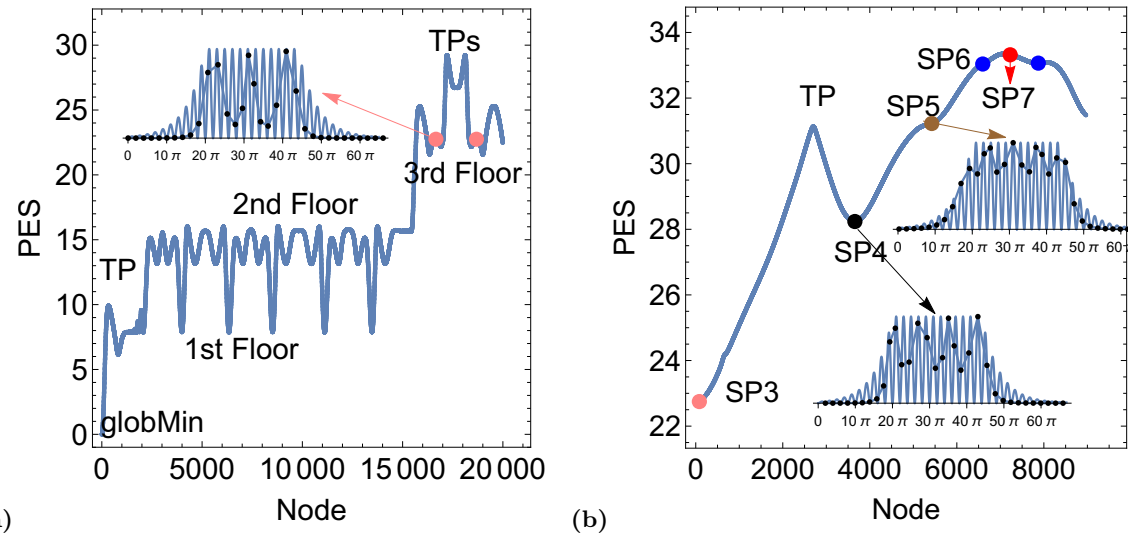

Fig. 29. (a) Profile over an NT to a pull-direction $(19\times0,\ 5\times1,\ 9\times0)^T$ connecting four energy levels of the Wigner chain. Two points representing the SP_3 are depicted by a pink bullet. The corresponding chain is the inset. (b) Profile over an NT from SP_3 over the 'global' SP_7, see Fig. 28 centre, here as a red bullet. The search direction of the NT is the 5th eigenvector of the SP_3. Blue are two SP_6 which are slightly unsymmetrical but which are vice versa symmetric, and brown is an SP_5. An SP_4 is a black bullet; the last two are shown in the insets. All SPs from index 3 to 6 are slightly unsymmetrical. The 'global' SP_7 is a single peak of the PES surrounded by SPs of lower index; thus this is a 'highest floor' as well. Intermediate minimums apparently do not exist.

and finally rises further up to the third floor where only one SP_3 exists with a 'triple'-state of kink-antikink-kink character which is shown in the inset of Fig. 29(a). Further stationary points of index 3 possibly seem not to fit into the only 11 full dimples of the 33-chain, on this 3rd floor. Of course, for a longer chain further corresponding floors will exist.

We add a remark to the usefulness or not of SPs of a higher index [25,58]. They are instable structures not only for the one direction where the chain propagates, like the SPs of index 1, but also for directions across the propagation direction. One can imagine an SP_2 being a summit on a 2D landscape. So, any fluctuation in the structure will lead to a 'falling down' to a lower level of the PES. These lower levels of the PES we determine by the tool of NTs, but one can use any other optimization tool. For example, one can use the minimization in Mma.

We gave an example in ref. [26] with the PES of a 23-particles chain, where an MEP and a quasi parallel LEP exist. In between is an SP_2 with a Figure for illustration.

Fig. 29b shows the energy profile of a further NT which explores the uppermost floor of the PES. The search direction of the NT is the 5th eigenvector of the SP_3 of the 3rd floor. The NT nicely connects all SPs with an increasing index up to the 'global' SP_7 at the top. It illustrates the index-theorem for NTs that they connect stationary points of an index difference of one [52].

9 Dynamics of the fully equal external force

The symmetric external excitation with an equal force to all electrons, the force $(1,...,1)^T$ is often used in experiments [17,18]. In this case with the very weak $k = 1$, the external force does not work well for an NT. For the side-potential with damping this equal force does not act equally on all particles because of the damped dimples at the two peripheries. They 'feel' the force more directly than the inner particles which are embedded in their deeper dimples.

Many NT calculations with this force and similar ones are done. We have to report that the NTs starting at the global minimum do not reach the central region of the chain. They compress electrons on the left hand side in the damped dimples region, and they pull electrons on the right hand side to a kink, but they stop at energies over 14 units at a 'clash-point' (by unknown, probably numerical reasons).

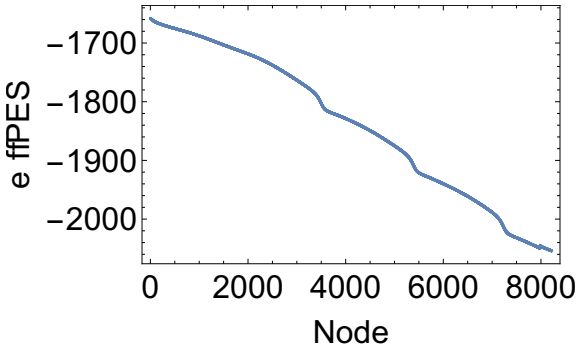

Fig. 30. k=1: profile of the effective energy over a Langevin solution.

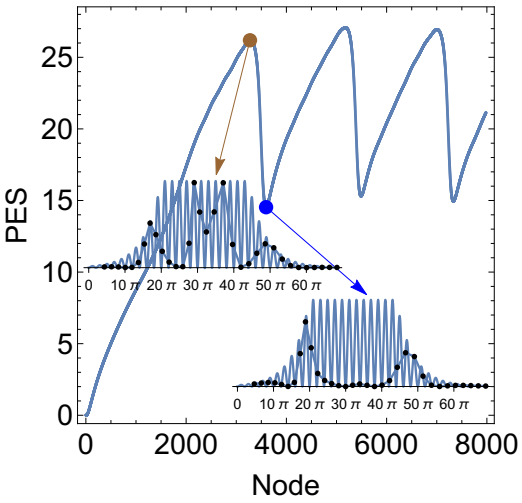

Fig. 31. k=1: profile of the energy over a Langevin solution without the external energy.

Another test with a start on the second floor also could not find the way out of the floor. So, we change here again to a treatment with the dynamical Langevin equation (14).

For a solution of the Langevin equation (14) we start at the global minimum and apply the external force to unit direction. The force amount $F = 0.5$ is again large enough to get the tilted effective PES where the chain slides downhill. For the differential equation (14) we use the step length of 0.01 units, and get the profile of the steepest descent ansatz in Fig. 30. Again, the sliding goes continuesly downhill, but with different slope.

The profile without the pure tilting part is shown in Fig. 31. Like in the case $k = 8$ we here find a strong increase of the energy at the start: the search direction is fully symmetric, and some steps after leaving the minimum one is on a ridge of the PES. It goes up into the region of the third floor. We show the structure of the chain at the first maximal energy of the PES in an inlay. There it deviates from the ridge and falls down but only into the region of the second floors. The next minimal structure is also shown in Fig. 31 by an inlay. The next cycles iterate downhill on the effective PES of Fig. 30 in the same region of Fig. 31. If we do not know the diverse valleys of the PES then we could not understand these cycles.

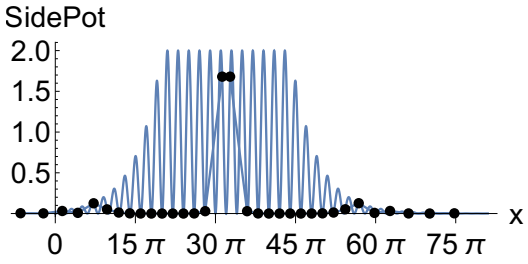

Fig. 32. A kink SP for a structure with Coulomb force for the springs of the chain, see text.

10 Discussion

We mostly treat a static PES model of the WS of a chain of electrons. On this PES we look for low pathways for a movement of kinks or antikinks of the chain. We do not describe the real, dynamical movement of such quasiparticles. We only calculate by NTs possible pathways over low SPs and depict special structures of the chain on such pathways. Using the Langevin equation, we treat a quasi-dynamical, damped descent on the effective PES. We assume a separation of dimples which we fix, and of quick single electrons in the kinks or antikinks. So to say we activate a former 'rigid-potential sliding model' of the WS [41].

Since only a kink or an antikink moves in our model, but the remaining electrons stay in their corresponding dimple, we must not assume that the DL disappears under a sliding, in contrast to former assumptions for a collective sliding of the chain [41]. But of course such a structure of a stable DL needs a chain of a certain length.

We do not take into account the phonons of the WS which emerge in phase with the DL, or out of phase. We only sometimes use the eigenvector directions of the Hessian of stationary points of the PES for search directions of the NTs.

To justify the transformation of the WS to an FK model we add a test calculation for an extremal structure with the correct Coulomb force formula Eq. (1). Note that this formula does not contain the constant a_o which has defined an equilibrium distance in the chain. Here such a distance does not exist. In the model, only the peaks and troughs of the dimples hold together the chain. The resulting structure in Fig.32 is a kink-SP. Thus analogous structures like under the harmonic force potential may exist. The used factor for the dimples is v=2 and for the spring force it is k_C=8. We optimized in Mathematica a former SP_1 of the other force of Eq.(8). Note that at the periphery the 'unbounded' Coulomb force moves the electrons far away! We wonder that the outer particles are not moved to infinity in this abstract mathematical model.

To include directly the electron density into a spring formula for the Coulomb forces seems to be difficult. Both reservoirs before and after the channel for the chain, in the experiments [17,18], are a constellation which presses the Coulomb forces into a pattern. But these boundary conditions destroy an FK model of a finite, but freely moving chain. On the other hand, we gave a comment on fixed boundary conditions in a former paper [25]. And finally, we will move the full chain. Thus we cannot fix the outer electrons.

Note that the density of electrons in a semiconductor or a metal is quite higher [59]. We do not consider excited states of the electrons here. Electronic properties of an FK model are discussed elsewhere [60], however, for a different misfit relation than we treat it.

We also do not consider the possibility that the WS can deviate in the plane from its quasi 1D shape to form a zigzag chain [61–64]. In the case of a linear chain treated here there is no possibility that a single electron moves. The interaction of the particles in the chain lead to collective states like kinks or antikinks.

11 Conclusions

We apply the model of an FK chain to a WS. Although conceptually simple, the model displays extremely rich physics. We compute the response of the FK chain to a linear external excitation. The static enlightenment of the low energy pathways of the PES of a WS chain allows us to propose an understanding of the experiments done with a quasi 1D chain of a WS. If an external force shifts the chain structure up to a first 'floor' of the PES then a kink, or an antikink in the chain will slide along this floor, independent on the length of the chain, and it can fall back at the end into a next global minimum with an off-radiation of the stored energy. It causes a movement of the full chain by the periodicity, a_s, of the dimple lattice. For the strong spring potential with $k = 8$ we already summarized some conclusions in Section 7 in Part I. For the weak springs with $k = 1$ in Part II the floors become somewhat less flat; they have distinguishable SPs and intermediate minimums on the floor level. However, the global behavior is similar.

With the length of the kinks or the antikinks in the two cases, k=8 and k=1, and an additional calculation with k=16 (not reported above), we can approximate the length of kinks or antikinks, L, for a general ratio of the potentials to be

$$L \approx 8 \sqrt{\frac{k}{v}} \ . \tag{15}$$

The right hand side formula was reported elsewhere [45] from the sine-Gordon equation with the slightly smaller factor a_s insteed of 8. Because the energy of the kinks or antikinks is directly connected with the length of the corresponding collective state, we can approximate the energy by a similar formula

$$V \approx 11.25 \sqrt{\frac{k}{v}} \ . \tag{16}$$

If a kink or an antikink hovers over the tops of the full dimples, nearly without additional energy effort, then we observe a density change of the chain in kind of a wave, and because the electrons have a charge, one could name the process "charge-density wave" [41,65]. Of course, the name is used in metals or semiconductors with another meaning [66–68], however, our highly idealized picture of the FK model may be used also to lighten such processes. And it may hold that also these charge-density waves here are the simplest patterns of moving configurations of electrons.

Declarations

Funding
We acknowledge the financial support from the Spanish Ministerio de Economía y Competitividad, Project PID 2019-109518GB-I00, Spanish Structures of Excellence María de Maeztu program, grant MDM-2017-0767 and Generalitat de Catalunya, project 2017 SGR 348.

Conflicts of interest
There is no conflict of competing interests.

Availability of data
Data of all stationary states reported in the paper are available on request by WQ.

Code
The Fortran code for the following of an NT, as well as the parallel Mathematica codes for the calculation of stationary points of the WS, and representation of the Figures are available on request by WQ.

Authors' contributions
We thank Katerchen, the cat, for helping us randomize the order of all authors who contributed equally to the manuscript.

References

1. I. Shapir, A. Hamo, S. Pecker, C.P. Moca, Ö. Legeza, G. Zarand, S. Ilani, Science **364**, 870 (2019)
2. C.C. Grimes, G. Adams, Phys. Rev. Lett. **42**, 795 (1979)
3. D.S. Fisher, B.I. Halperin, P.M. Platzman, Phys. Rev. Lett. **42**, 798 (1979)
4. E.Y. Andrei (ed.), *Two-Dimensional Electron Systems on Helium and other Cryogenic Substrates*, Physics and Chemistry of Materials with Low-Dimensional Structures (PCMALS, vol. 19) (Springer, Berlin, 1997)
5. M.I. Dykman, C. Fang-Yen, M.J. Lea, Phys. Rev. B **55**, 16249 (1997)
6. Y.P. Monarkha, K. Kono, *Two-Dimensional Coulomb Liquids and Solids* (Springer, Berlin, 2004)

7. G.F. Giuliani, G. Vignale, *Quantum Theory of the Electron Liquid* (Cambridge University Press, Cambridge, 2005)
8. J. Klier, I. Doicescu, P. Leiderer, J. Low Temp. Phys. **121**, 603 (2000)
9. P. Glasson, S.E. Andresen, G. Ensell, V. Dotsenko, W. Bailey, P. Fozooni, A. Kristensen, M.J. Lea, Physica B **284-288**, 1916 (2000)
10. H. Ikegami, H. Akimoto, K. Kono, Phys. Rev. B **82**, 201104 (2010)
11. H. Ikegami, H. Akimoto, D.G. Rees, K. Kono, Phys. Rev. Lett. **109**, 236802 (2012)
12. D.G. Rees, H. Ikegami, K. Kono, J. Phys. Soc. Jpn. **82**, 124602 (2013)
13. D.G. Rees, N.R. Beysengulov, J.J. Lin, K. Kono, Phys. Rev. Lett. **116**, 206801 (2016)
14. M.I. Dykman, Physics **9**, 54 (2016)
15. D.G. Rees, S.S. Yeh, B.C. Lee, K. Kono, J.J. Lin, Phys. Rev. B **96**, 205438 (2017)
16. A.O. Badrutdinov, A.V. Smorodin, D.G. Rees, J.Y. Lin, D. Konstantinov, Phys. Rev. B **94**, 195311 (2016)
17. J.Y. Lin, A.V. Smorodin, A.O. Badrutdinov, D. Konstantinov, Phys. Rev. B **98**, 085412 (2018)
18. J.Y. Lin, A.V. Smorodin, A.O. Badrutdinov, D. Konstantinov, J. Low Temp. Phys. **195**, 289 (2019)
19. Y.P. Monarkha, Europ. Phys. Lett. **118**, 67001 (2017)
20. Y.P. Monarkha, K. Kono, J. Phys. Soc. Jpn. **74**, 960 (2005)
21. W.F. Vinen, J. Phys.: Condens. Matter **11**, 9709 (1999)
22. M.I. Dykman, Y.G. Rubo, Phys.Rev. Lett. **78**, 4813 (1997)
23. H.J. Lauter, H. Godfrin, V.L.P. Frank, P. Leiderer, Phys. Rev. Lett. **68**, 2484 (1992)
24. D.G. Rees, I. Kuroda, C.A. Marrache-Kikuchi, M. Hoefer, P. Leiderer, K. Kono, Phys. Rev. Lett. **106**, 026803 (2011)
25. W. Quapp, J.M. Bofill, Molec. Phys. **117**, 1541 (2019)
26. W. Quapp, J.M. Bofill, European Phys. J. B **92**, 95 (2019)
27. W. Quapp, J.M. Bofill, European Phys. J. B **92**, 193 (2019)
28. H.J. Schulz, J. Phys. C **16**, 6769 (1983)
29. W. Quapp, J.M. Bofill, Theoret. Chem. Acc. **135**, 113 (2016)
30. W. Quapp, J.M. Bofill, J. Ribas-Ariño, Int. J. Quant. Chem. **118**, e25775 (2018)
31. J.M. Bofill, J. Ribas-Ariño, S.P. García, W. Quapp, J. Chem. Phys. **147**, 152710 (2017)
32. W. Quapp, J.M. Bofill, Int. J. Quant. Chem. **118**, e25522 (2018)
33. D.A. Gangloff, A. Bylinskii, V. Vuletić, Phys. Rev. Research **2**, 013380 (2020)
34. K.M. Yunusova, D. Konstantinov, H. Bouchiat, A.D. Chepelianskii, Phys. Rev. Lett. B **94**, 195311 (2016)
35. O.V. Zhirov, J. Lages, D.L. Shepelyansky, Euro. Phys. J. D **73**, 149 (2019)
36. M.Y. Zakharov, D. Demidov, D.L. Shepelyansky, arXiv1901.05231 (2019)
37. V.Y. Sivokon, Low Temp.Phys. **45**, 58 (2019)
38. H. Ikegami, H. Akimoto, K. Kono, J. Phys. Conf. Series **400**, 012020 (2012)
39. K. Shirahama, K. Kono, Phys. Rev. Lett. **74**, 781 (1995)
40. H. Ikegami, H. Akimoto, K. Kono, Phys. Rev. Lett. **102**, 046807 (2009)
41. K. Shirahama, K. Kono, J. Low Temp. Phys. **104**, 237 (1996)
42. Y.P. Monarkha, K. Kono, Low Temp. Phys. **35**, 356 (2009)
43. O.M. Braun, B. Hu, A. Zeltser, Phys. Rev. E **62**, 4235 (2000)
44. I.D. Mikheikin, M.Y. Kuznetsov, E.V. Makhonina, V.S. Pervov, J. Mater. Synth. Process. **10**, 53 (2002)
45. O.M. Braun, Y.S. Kivshar, M. Peyrard, Phys. Rev. E **56**, 6050 (1997)
46. J.I. Frenkel, *Wave Mechanics. Elementary Theory* (Clarendon Press, Oxford, 1932)
47. M. Peyrard, M.D. Kruskal, Physica D **14**, 88 (1984)
48. C. Yannouleas, U. Landman, Rep. Progr. Phys. **70**, 2067 (2007)
49. J. Odavić, P. Malik, J. Tekić, M. Pantić, M. Pavkov-Hrvojević, Commun. Nonlinear Sci. Numer. Simulat. **47**, 100 (2017)
50. J. Tekić, D. He, B. Hu, Phys. Rev. E **79**, 036604 (2009)
51. S.V. Dmitriev, L.V. Nauman, A.M. Wusatowska-Sarnek, M.D. Starostenkov, phys. stat. sol. (b) **201**, 89 (1997)
52. M. Hirsch, W. Quapp, J. Molec. Struct., THEOCHEM **683**, 1 (2004)
53. G.A. Csáthy, D.C. Tsui, L.N. Pfeiffer, K.W. West, Phys. Rev. Lett. **98**, 066805 (2007)
54. J. Tekić, A.E. Botha, P. Mali, Y.M. Shukrinov, Phys. Rev. E **99**, 022206 (2019)
55. M. Hirsch, W. Quapp, Chem. Phys. Lett. **395**, 150 (2004)
56. A.B. Kolton, A. Rosso, T. Giamarchi, W. Krauth, Phys. Rev. Lett. **97**, 057001 (2006)
57. S. Aubry, Physica **7D**, 240 (1983)
58. D. Heidrich, W. Quapp, Theor. Chim. Acta **70**, 89 (1986)
59. Y.P. Monarkha, V.E. Syvokon, Low Temp. Phys. **38**, 1067 (2012)
60. P. Tong, B. Li, B. Hu, Phys. Rev. Lett. **88**, 046804 (2002)
61. P.L. Christiansen, A.V. Savin, A.V. Zolotaryuk, Phys. Rev. B **54**, 12892 (1996)
62. A.D. Klironomos, J.S. Meyer, K.A. Matveev, EuroPhys. Lett. **74**, 679 (2006)
63. V.E. Syvokon, S.S. Sokolov, Low Temp. Phys. **41**, 858 (2015)
64. J.B. Okaly, F. II Ndzana, R.L. Woulaché, T.C. Kofané, Eur. Phys. J. Plus **134**, 598 (2019)
65. H.J. Schulz, Phys. Rev. Lett. **71**, 1864 (1993)
66. G. Grüner, Rev. Mod. Phys. **60**, 1129 (1988)
67. R. Thorne, Physics Today **1996**, 42 (1996)
68. J.P. Pouget, C. R. Physique **17**, 332 (2016)